Transverse Target Moments of Dihadron Production in Semi-inclusive Deep Inelastic Scattering at HERMES

S. Gliske

University of Michigan / HERMES Collaboration

Doctoral Dissertation Defense
267B West Hall
Ann Arbor, Michigan
April 11$^{\text{th}}$, 2011

Outline

Motivation & Background

Fragmentation

- An important, open issue in QCD is the nature of confinement
  - Confinement is the statement that quarks never exist as free particles in nature.
  - Related to the strong force being negligible at short distances and extremely strong at larger distances (10^{-15} m)
  - Confinement causes any quark attempting to exit a bound state to either be pulled back into the bound state or to hadronize into a new particle.
- Fragmentation is the process by which a quark hadronizes into the observed particles.
  - The original bound state is said to "fragment"
- Two types of fragmentation are usually defined

  Favored: struck quark present in the observed particles.

  Disfavored: struck quark not present in the observed particles.

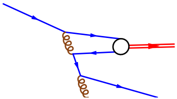

- One of the key issues of this dissertation is the transverse momentum dependent (TMD) spin-structure of fragmentation.

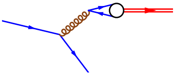

- Note: TMD effects also important aspect of proton structure.

SIDIS Production of Hadrons

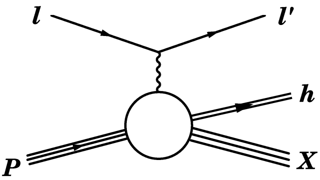

- The SIDIS hadron & dihadron processes

$$
\begin{aligned}
e + p &\rightarrow e' + h + X, \\
e + p &\rightarrow e' + h_1 + h_2 + X.
\end{aligned}
$$

- Dihadron production includes all subprocesses leading to hadron pair final states

- Factorization theorem implies $\sigma^{ep\rightarrow ehX} = \sum_q DF \otimes \sigma^{eq\rightarrow eq} \otimes FF$
- Access integrals of DFs and FFs through Fourier moments of ϕ_h, ϕ_S, ϕ_R & Legendre polynomials in $\cos\vartheta$.

$$
\begin{aligned}
\phi_h &= \operatorname{signum}\left[(\boldsymbol{k} \times \boldsymbol{P}_h) \cdot \boldsymbol{q} \right] \arccos \frac{(\boldsymbol{q} \times \boldsymbol{k}) \cdot (\boldsymbol{q} \times \boldsymbol{P}_h)}{|\boldsymbol{q} \times \boldsymbol{k}| \, |\boldsymbol{q} \times \boldsymbol{P}_h|}, \\
\phi_S &= \operatorname{signum}\left[(\boldsymbol{k} \times \boldsymbol{S}) \cdot \boldsymbol{q} \right] \arccos \frac{(\boldsymbol{q} \times \boldsymbol{k}) \cdot (\boldsymbol{q} \times \boldsymbol{S})}{|\boldsymbol{q} \times \boldsymbol{k}| \, |\boldsymbol{q} \times \boldsymbol{S}|}, \\
\phi_R &= \operatorname{signum}\left[(\boldsymbol{R} \times \boldsymbol{P}_h) \cdot \boldsymbol{n} \right] \arccos \frac{(\boldsymbol{q} \times \boldsymbol{k}) \cdot (\boldsymbol{P}_h \times \boldsymbol{R})}{|\boldsymbol{q} \times \boldsymbol{k}| \, |\boldsymbol{P}_h \times \boldsymbol{R}|}.
\end{aligned}
$$

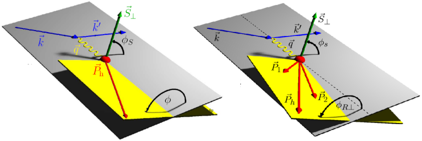

The HERMES Spectrometer

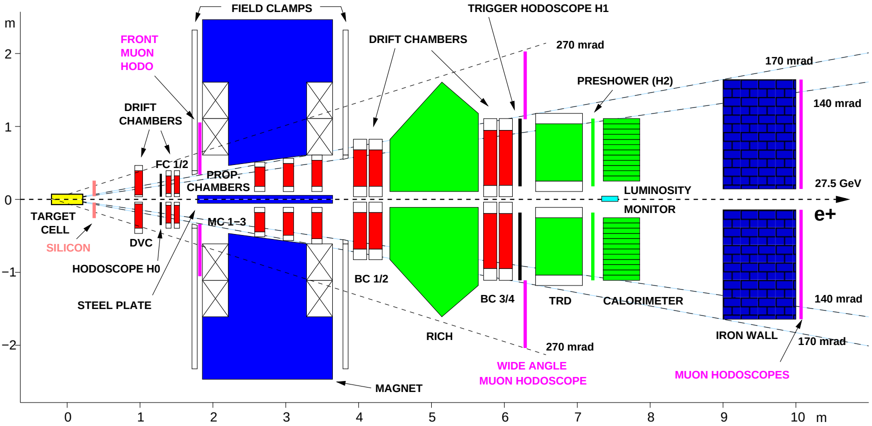

Beam Long. pol. $e^{\pm}$ at 27.6 GeV

Target Trans. pol. H ($\approx$ 75%)
Log. pol. H ($\approx$ 85%)
Unpol. H,D,Ne,Kr,. . .

Lep.-Had. Sep. High efficiency $\approx$ 98%
Low contamination (<2%)

Hadron PID Separates $\pi^{\pm}$, $K^{\pm}$, p, $\bar{p}$
with momenta in 2-15 GeV

Collinear Dihadron Results

HERMES

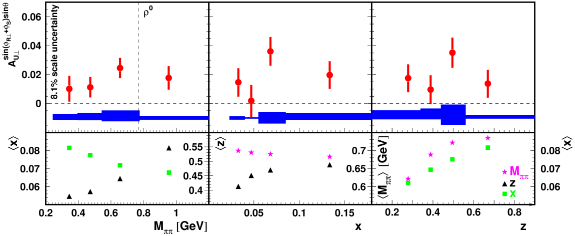

COMPASS

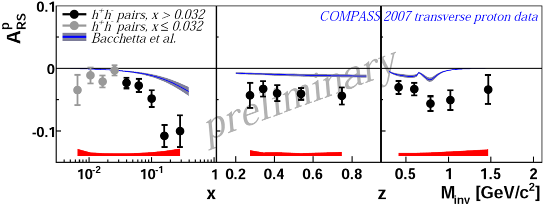

- Measure asymmetry $2\,\langle \sin(\phi_{R\perp} + \phi_S) \sin\theta \rangle$ in $\pi^+\pi^-$ pair production.
- Related to h_1 DF (transversity) and *sp* interference FF $H_{1,UT}^{\sphericalangle sp}$.
- Model based on HERMES results by Bacchetta, *et al.* (PRD 74:114007, 2006)
- Prediction for COMPASS results yields too small of an asymmetry. (arXiv:0907.0961v1)
- Both experiments indicate non-zero h_1 and $H_{1,UT}^{\sphericalangle sp}$.

Lund/Artru String Fragmentation Model

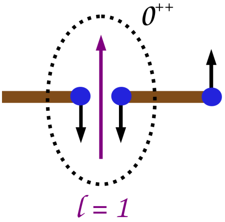

- Favored fragmentation modeled as the breaking of a gluon flux tube between the struck quark and the remnant.
- Assume that the flux tube breaks into a $q\bar{q}$ pair with quantum numbers equal to the vacuum.

- Expect mesons overlapping with $|\frac{1}{2},\frac{1}{2}\rangle|\frac{1}{2},-\frac{1}{2}\rangle$ and $|\frac{1}{2},-\frac{1}{2}\rangle|\frac{1}{2},\frac{1}{2}\rangle$ states to prefer "quark left".
  - $|0,0\rangle =$ pseudo-scalar mesons.
  - $|1,0\rangle =$ longitudinally polarized vector mesons.
- Expect mesons overlapping with $|\frac{1}{2},\frac{1}{2}\rangle|\frac{1}{2},\frac{1}{2}\rangle$ and $|\frac{1}{2},-\frac{1}{2}\rangle|\frac{1}{2},-\frac{1}{2}\rangle$ states to prefer "quark right".
  - $|1,\pm1\rangle =$ transversely polarized vector mesons.
- For the two ρ_T's, "the Collins function" should have opposite sign to that for π
- For ρ_L, "the Collins function" is zero.

Lund/Artru String Fragmentation Model

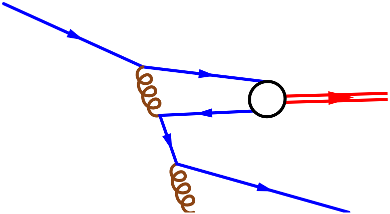

- Favored fragmentation modeled as the breaking of a gluon flux tube between the struck quark and the remnant.
- Assume that the flux tube breaks into a $q\bar{q}$ pair with quantum numbers equal to the vacuum.

- Expect mesons overlapping with $|\frac{1}{2},\frac{1}{2}\rangle|\frac{1}{2},-\frac{1}{2}\rangle$ and $|\frac{1}{2},-\frac{1}{2}\rangle|\frac{1}{2},\frac{1}{2}\rangle$ states to prefer "quark left".
  - $|0,0\rangle =$ pseudo-scalar mesons.
  - $|1,0\rangle =$ longitudinally polarized vector mesons.
- Expect mesons overlapping with $|\frac{1}{2},\frac{1}{2}\rangle|\frac{1}{2},\frac{1}{2}\rangle$ and $|\frac{1}{2},-\frac{1}{2}\rangle|\frac{1}{2},-\frac{1}{2}\rangle$ states to prefer "quark right".
  - $|1,\pm 1\rangle =$ transversely polarized vector mesons.
- For the two ρ_T's, "the Collins function" should have opposite sign to that for π
- For ρ_L, "the Collins function" is zero.

Gluon Radiation Fragmentation Model

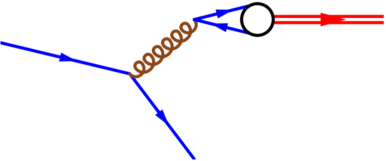

- Disfavored frag. model: assume produced diquark forms the observed meson
- Assume additional final state interaction to set pseudo-scalar quantum numbers
- Assume no additional interactions in dihadron production.

- Exists common sub-diagram between this model and the Lund/Artru model.
- Keeping track of quark polarization states, sub-diagram for disfavored $|1,1\rangle$ diquark production identical to sub-diagram for favored $|\frac{1}{2},-\frac{1}{2}\rangle|\frac{1}{2},\frac{1}{2}\rangle$ diquark production.

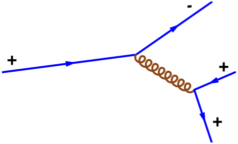

- Implies that the disfavored Collins function for transverse vector mesons also has opposite sign as the favored pseudo-scalar Collins function
- Data suggests fav. and disfav. Collins functions for pseudo-scalars are approx. equal and opposite, while these theories suggest fav. and disfav. Collins functions for transverse vector mesons are approx. equal.

HERMES Collins Moments for Pions

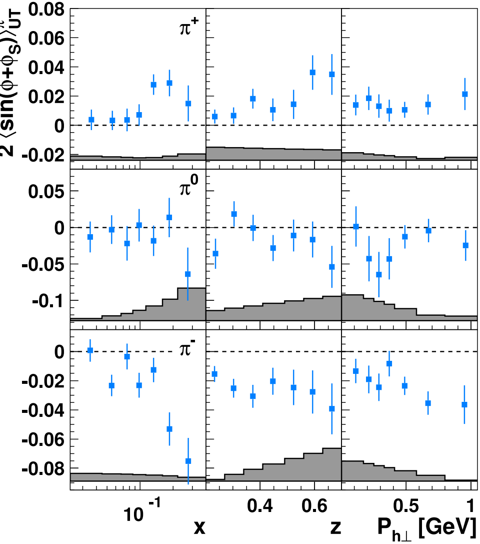

- Final result published in January
  A. Airapetian et al, Phys. Lett. B 693 (2010) 11-16. arXiv:1006.4221 (hep-ex)
- Significant π^- asymmetry implies $H_1^{\perp,disf} \approx -H_1^{\perp,fav}$
- Pions have small, but non-zero asymmetry
- Expect Collins moments negative for $\rho^\pm$.
- Would like uncertainties on dihadron moments on the order of 0.02.

Theory

Fragmentation Functions and Spin/Polarization

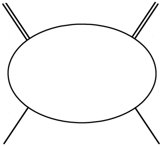

- Leading twist Fragmentation functions are related to number densities
  - Amplitudes squared rather than amplitudes
- Difficult to relate Artru/Lund prediction with published notation and cross section.
- Propose new convention for fragmentation functions
  - Functions entirely identified by the polarization states of the quarks, χ and χ'
  - Any final-state polarization, i.e. $|\ell_1, m_1\rangle|\ell_2, m_2\rangle$, contained within partial wave expansion of fragmentation functions
- Exists exactly two fragmentation functions
  - D_1, the unpolarized fragmentation function ($\chi = \chi'$)
  - $H_1^{\perp}$, the polarized (Collins) fragmentation function ($\chi \neq \chi'$)
- New partial waves analysis proposed, using direct sum basis $|\ell, m\rangle$ rather than the direct product basis $|\ell_1, m_1\rangle|\ell_2, m_2\rangle$.

Partial Wave Expansion

- Fragmentation functions expanded into partial waves in the direct sum basis according to

$$
\begin{aligned}
D_1 &= \sum_{\ell=1}^{\infty} \sum_{m=-\ell}^{\ell} P_{\ell,m}(\cos\vartheta) e^{im(\phi_R-\phi_k)} D_1^{|\ell,m\rangle}(z, M_h, |\boldsymbol{k}_T|), \\
H_1^{\perp} &= \sum_{\ell=1}^{\infty} \sum_{m=-\ell}^{\ell} P_{\ell,m}(\cos\vartheta) e^{im(\phi_R-\phi_k)} H_1^{\perp|\ell,m\rangle}(z, M_h, |\boldsymbol{k}_T|),
\end{aligned}
$$

- Each term in pseudo-scalar and dihadron cross section uniquely related to a specific partial wave $|\ell, m\rangle$.
- Cross section looks the same for all final states, excepting certain partial waves may or may not be present
  - Pseudo-scalar production is $\ell = 0$ sector
  - Dihadron production is $\ell = 0, 1, 2$ sector
  - Given the pseudo-scalar cross section (at any twist) can extrapolate cross section for other final states

Where is “the Collins function” for Vector Mesons?

- Consider direct sum vs. direct product basis

$$\frac{1}{2}\otimes\frac{1}{2}\otimes\frac{1}{2}\otimes\frac{1}{2} = \left(\frac{1}{2}\otimes\frac{1}{2}\right)\otimes\left(\frac{1}{2}\otimes\frac{1}{2}\right), = (1\oplus 0)\otimes(1\oplus 0), = 2\oplus 1\oplus 1\oplus 1\oplus 0\oplus 0.$$

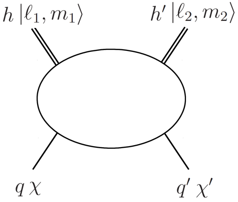

- Three $\ell = 1$ and two $\ell = 0$ cannot be separated experimentally
  - Theoretically distinguishable via Generalized Casimir Operators
- Longitudinal vector meson state $|1,0\rangle|1,0\rangle$ is a mixture of $|2,0\rangle$ and $|0,0\rangle$
  - Cannot access, due to $\ell = 0$ multiplicity
  - Model predictions for longitudinal vector mesons not testable
- Transverse vector meson states $|1,\pm1\rangle|1,\pm1\rangle$ are exactly $|2,\pm2\rangle$
  - Models predict dihadron $H_1^{\perp|2,\pm2\rangle}$ has opposite sign as pseudo-scalar $H_1^{\perp}$.
  - Cross section has direct access to $H_1^{\perp|2,\pm2\rangle}$

Dihadron Twist-3 Cross Section

$$
\begin{aligned}
d\sigma_{UU} &= \frac{\alpha^2 M_h P_{h\perp}}{2\pi x y Q^2}\left(1+\frac{\gamma^2}{2x}\right) \\
&\times \sum_{\ell=0}^{2}\Bigg\{ A(x,y)\sum_{m=0}^{\ell}\Big[P_{\ell,m}\cos(m(\phi_h-\phi_R))\Big(F_{UU,T}^{P_{\ell,m}\cos(m(\phi_h-\phi_R))}+\epsilon F_{UU,L}^{P_{\ell,m}\cos(m(\phi_h-\phi_R))}\Big)\Big] \\
&\quad + B(x,y)\sum_{m=-\ell}^{\ell}P_{\ell,m}\cos((2-m)\phi_h+m\phi_R)F_{UU}^{P_{\ell,m}\cos((2-m)\phi_h+m\phi_R)} \\
&\quad + V(x,y)\sum_{m=-\ell}^{\ell}P_{\ell,m}\cos((1-m)\phi_h+m\phi_R)F_{UU}^{P_{\ell,m}\cos((1-m)\phi_h+m\phi_R)}\Bigg\},
\end{aligned}
$$

$$
\begin{aligned}
d\sigma_{UT} &= \frac{\alpha^2 M_h P_{h\perp}}{2\pi x y Q^2}\left(1+\frac{\gamma^2}{2x}\right)|\boldsymbol{S}_\perp|\sum_{\ell=0}^{2}\sum_{m=-\ell}^{\ell}\Bigg\{A(x,y)\Big[P_{\ell,m}\sin((m+1)\phi_h-m\phi_R-\phi_S)) \\
&\quad\times\Big(F_{UT,T}^{P_{\ell,m}\sin((m+1)\phi_h-m\phi_R-\phi_S)}+\epsilon F_{UT,L}^{P_{\ell,m}\sin((m+1)\phi_h-m\phi_R-\phi_S)}\Big)\Big] \\
&\quad + B(x,y)\Big[P_{\ell,m}\sin((1-m)\phi_h+m\phi_R+\phi_S)F_{UT}^{P_{\ell,m}\sin((1-m)\phi_h+m\phi_R+\phi_S)} \\
&\qquad + P_{\ell,m}\sin((3-m)\phi_h+m\phi_R-\phi_S)F_{UT}^{P_{\ell,m}\sin((3-m)\phi_h+m\phi_R-\phi_S)}\Big] \\
&\quad + V(x,y)\Big[P_{\ell,m}\sin(-m\phi_h+m\phi_R+\phi_S)F_{UT}^{P_{\ell,m}\sin(-m\phi_h+m\phi_R+\phi_S)} \\
&\qquad + P_{\ell,m}\sin((2-m)\phi_h+m\phi_R-\phi_S)F_{UT}^{P_{\ell,m}\sin((2-m)\phi_h+m\phi_R-\phi_S)}\Big]\Bigg\}.
\end{aligned}
$$

Structure Functions, Unpolarized

$$F_{UU,L}^{P_{\ell,m}\cos(m\phi_h - m\phi_R)} = 0,$$

$$F_{UU,T}^{P_{\ell,m}\cos(m\phi_h - m\phi_R)} = \begin{cases} \mathcal{I}\left[f_1 D_1^{|\ell,0\rangle}\right] & m = 0, \\ \mathcal{I}\left[2\cos(m\phi_h - m\phi_k)\, f_1 \left(D_1^{|\ell,m\rangle} + D_1^{|\ell,-m\rangle}\right)\right] & m > 0, \end{cases}$$

$$F_{UU}^{P_{\ell,m}\cos((2-m)\phi_h + m\phi_R)} = -\mathcal{I}\left[\frac{|\boldsymbol{p}_T||\boldsymbol{k}_T|}{MM_h}\cos\left((m-2)\phi_h + \phi_p + (1-m)\phi_k\right) h_1^\perp H_1^{\perp|\ell,m\rangle}\right],$$

$$F_{UU}^{P_{\ell,m}\cos((1-m)\phi_h + m\phi_R)} = -\frac{2M}{Q}\mathcal{I}\left[\frac{|\boldsymbol{k}_T|}{M_h}\cos((m-1)\phi_h + (1-m)\phi_k) \times \left(xhH_1^{\perp|\ell,m\rangle} + \frac{M_h}{M} f_1 \frac{\tilde{D}^{\perp|\ell,m\rangle}}{z}\right) + \frac{|\boldsymbol{p}_T|}{M}\cos((m-1)\phi_h + \phi_p - m\phi_k) \times \left(xf^\perp D_1^{|\ell,m\rangle} + \frac{M}{M_h} h_1^\perp \frac{\tilde{H}^{|\ell,m\rangle}}{z}\right)\right].$$

- Can test Lund/Artru model with $F_{UU}^{\sin^2\vartheta\cos(2\phi_R)}$, $F_{UU}^{\sin^2\vartheta\cos(4\phi_h - 2\phi_R)}$ via Boer-Mulder's function

Twist-2 Structure Functions, Transverse Target

$$F_{UT,L}^{P_{\ell,m}\sin((m+1)\phi_h - m\phi_R - \phi_S)} = 0$$

$$F_{UT,T}^{P_{\ell,m}\sin((m+1)\phi_h - m\phi_R - \phi_S)} = -\mathfrak{I}\left[\frac{|\boldsymbol{p}_T|}{M}\cos\left((m+1)\phi_h - \phi_p - m\phi_k\right) \times \left(f_{1T}^{\perp}\left(D_1^{|\ell,m\rangle} + D_1^{|\ell,-m\rangle}\right) + \chi(m) g_{1T}\left(D_1^{|\ell,m\rangle} - D_1^{|\ell,-m\rangle}\right)\right)\right],$$

$$F_{UT}^{P_{\ell,m}\sin((1-m)\phi_h + m\phi_R + \phi_S)} = -\mathfrak{I}\left[\frac{|\boldsymbol{k}_T|}{M_h}\cos\left((m-1)\phi_h - \phi_p - m\phi_k\right) h_1 H_1^{\perp|\ell,m\rangle}\right],$$

$$F_{UT}^{P_{\ell,m}\sin((3-m)\phi_h + m\phi_R - \phi_S)} = \mathfrak{I}\left[\frac{|\boldsymbol{p}_T|^2|\boldsymbol{k}_T|}{M^2 M_h}\cos\left((m-3)\phi_h + 2\phi_p - (m-1)\phi_k\right) h_{1T}^{\perp} H_1^{\perp|\ell,m\rangle}\right].$$

- Can test Lund/Artru model with $F_{UT}^{\sin^2\vartheta\,\sin(-\phi_h+2\phi_R+\phi_S)}$ and $F_{UT}^{\sin^2\vartheta\,\sin(3\phi_h-2\phi_R+\phi_S)}$ via transversity
- In theory, could also test Lund/Artru and gluon radiation models with $F_{UT}^{\sin^2\vartheta\,\sin(\phi_h+2\phi_R-\phi_S)}$ and $F_{UT}^{\sin^2\vartheta\,\sin(5\phi_h-2\phi_R-\phi_S)}$ via pretzelocity
- Data from SIDIS pseudo-scalar production indicate pretzelocity very small or possibly zero

Collinear Dihadron Spectator Model

- Based on Bacchetta/Radici spectator model for collinear dihadron production *Phys. Rev.* D74 (2006)
  - The SIDIS X is replaced with a single, on-shell, particle of mass $M_s \propto M_h$.
  - Assume one spectator for hadron pairs and vector mesons.
  - Integration over transverse momenta is performed before extracting fragmentation functions.
- One can use the same correlator to extract TMD fragmentation functions
  - One just needs to not integrate and follow the Dirac-matrix algebra and partial wave expansion.
  - Numeric studies show need for additional $\boldsymbol{k}_T$ cut-off.
- Original model intended for $\pi^+\pi^-$ pairs
  - Adding flavor dependence allows generalization to $\pi^+\pi^0$, $\pi^-\pi^0$ pairs.
  - Slight change to vertex function allows generalization to K^+K^- pairs.
  - Slight change to vertex function and allows generalization to K^+K^- pairs.
- Unfortunately, the model only includes partial waves of the Collins function for $\ell < 2$.

Numerical Methods

Smearing/Acceptance Effects

- Let $\boldsymbol{x}^{(T)}$ be true value of variables, $\boldsymbol{x}^{(R)}$ the reconstructed values
- A conditional probability $p\left(\boldsymbol{x}^{(R)}\middle|\,\boldsymbol{x}^{(T)}\right)$ relates the true PDF $p\left(\boldsymbol{x}^{(T)}\right)$ with the PDF of the reconstructed variables, $p\left(\boldsymbol{x}^{(R)}\right)$.
- Specific relation given by Fredholm integral equation

$$\begin{aligned} p\left(\boldsymbol{x}^{(R)}\right) &= \eta \int d^D\boldsymbol{x}^{(T)}\, p\left(\boldsymbol{x}^{(R)}\middle|\,\boldsymbol{x}^{(T)}\right) p\left(\boldsymbol{x}^{(T)}\right), \\ \frac{1}{\eta} &= \int d^D\boldsymbol{x}^{(R)} d^D\boldsymbol{x}^{(T)}\, p\left(\boldsymbol{x}^{(R)}\middle|\,\boldsymbol{x}^{(T)}\right) p\left(\boldsymbol{x}^{(T)}\right). \end{aligned}$$

- Can rewrite in terms of a smearing operator

$$\begin{aligned} \tilde{g}\left(\boldsymbol{x}^{(R)}\right) &= S\left[g(\boldsymbol{x}^{(T)})\right], \\ &= \int d^D\boldsymbol{x}^{(T)}\, p\left(\boldsymbol{x}^{(R)}\middle|\,\boldsymbol{x}^{(T)}\right) g\left(\boldsymbol{x}^{(T)}\right). \end{aligned}$$

- Fredholm equation is simply

$$p\left(\boldsymbol{x}^{(R)}\right) = S\left[\eta p\left(\boldsymbol{x}^{(T)}\right)\right].$$

Solution with Finite Basis and Integrated Squared Error

- Restrict to finite basis

$$\begin{aligned} \eta p\left(\boldsymbol{x}^{(T)}\right) &= \sum_i \alpha_i f_i\left(\boldsymbol{x}^{(T)}\right), \\ p\left(\boldsymbol{x}^{(R)} \middle| \boldsymbol{x}^{(T)}\right) &= \sum_{i,j} \Gamma_{i,j} f_i\left(\boldsymbol{x}^{(R)}\right) f_j\left(\boldsymbol{x}^{(T)}\right). \end{aligned}$$

- Determine parameters by minimizing the integrated squared error (ISE)

$$\begin{aligned} ISE_1 &= \int d^D\boldsymbol{x}^{(R)} d^D\boldsymbol{x}^{(T)} \left[p\left(\boldsymbol{x}^{(R)} \middle| \boldsymbol{x}^{(T)}\right) - \sum_{i,j} \Gamma_{i,j} f_i(\boldsymbol{x}^{(R)}) f_j(\boldsymbol{x}^{(T)})\right]^2, \\ ISE_2 &= \int d^D\boldsymbol{x}^{(R)} \left\{p\left(\boldsymbol{x}^{(R)}\right) - S\left[\eta p\left(\boldsymbol{x}^{(T)}\right)\right]\right\}^2. \end{aligned}$$

Numerical Solution

- Define/compute

$$
\begin{aligned}
F_{i,j} &= \int d^D\boldsymbol{x}^{(\boldsymbol{T})} f_i\left(\boldsymbol{x}^{(\boldsymbol{T})}\right) f_j\left(\boldsymbol{x}^{(\boldsymbol{T})}\right), \\
B_{i,j} &= \int d^D\boldsymbol{x}^{(\boldsymbol{R})} d^D\boldsymbol{x}^{(\boldsymbol{T})}\, p\left(\boldsymbol{x}^{(R)}\middle|\, \boldsymbol{x}^{(T)}\right) f_i\left(\boldsymbol{x}^{(\boldsymbol{R})}\right) f_j\left(\boldsymbol{x}^{(\boldsymbol{T})}\right), \\
&= V\int d^D\boldsymbol{x}^{(\boldsymbol{R})} d^D\boldsymbol{x}^{(\boldsymbol{T})}\, p_{MC}\left(\boldsymbol{x}^{(T)}, \boldsymbol{x}^{(R)}\right) f_i\left(\boldsymbol{x}^{(\boldsymbol{R})}\right) f_j\left(\boldsymbol{x}^{(\boldsymbol{T})}\right), \\
b_i &= \int d^D\boldsymbol{x}^{(R)} p\left(\boldsymbol{x}^{(R)}\right) f_i\left(\boldsymbol{x}^{(R)}\right), \\
&= \frac{V}{N_R}\sum_{k=1}^{N_R} f_i\left(\boldsymbol{x}^{(R,k)}\right),
\end{aligned}
$$

- ISEs reduce to the matrix equation

$$B^T F^{-1} B\boldsymbol{\alpha} = B^T F^{-1}\boldsymbol{b}.$$

- Assuming $(B^T F^{-1} B)$ and B are invertible, the solution for the given ISEs is

$$\boldsymbol{\alpha} = \left(B^T F^{-1} B\right)^{-1} B^T F^{-1}\boldsymbol{b} = B^{-1}\boldsymbol{b}.$$

Uncertainty Calculation

- Define

$$\left(C^{\boldsymbol{b}}\right)_{j,j'} = \frac{\delta_{j,j'}}{N_R - 1}\left[\frac{V^2}{N_R}\sum_{k=1}^{N_R} f_i^2\left(\boldsymbol{x}^{(R,k)}\right) - (b_i)^2\right],$$

$$\left(C^{B}\right)_{j,k;j',k'} = \frac{\delta_{j,j'}\delta_{k,k'}}{N_\epsilon - 1}\left[\frac{V^4}{N_\epsilon}\sum_{k=1}^{N_\epsilon} f_j^2\left(\boldsymbol{x}^{(M,k)}\right) f_k^2\left(\boldsymbol{x}^{(T,k)}\right) - (B_{j,k})^2\right],$$

$$C'^{(B)}_{i,i'} = \sum_{j,j'} C^{(B)}_{i,j;i',j'}\alpha_j\alpha_{j'}.$$

- The uncertainty on $\boldsymbol{\alpha}$ is then

$$C^{(\boldsymbol{\alpha})} = B^{-1}C^{(\boldsymbol{b})}B^{-T} + B^{-1}C'^{(B)}B^{-T}.$$

- One could consider a third term $\left(B^T F^{-1} B\right)^{-1}$, the Hessian of the matrix eq.
  - Numeric studies show this term is not a meaningful estimate of the uncertainty, and that it can be neglected.

New TMDGEN Generator

- No previous Monte Carlo generator has TMD dihadron production with full angular dependence
- Method
  - Integrates cross section per flavor to determine "quark branching ratios"
  - Throw a flavor type according to ratios
  - Throw kinematic/angular variables by evaluating cross section
    - Can use weights or acceptance rejection
  - Full TMD simulation: each event has specific $|\boldsymbol{p}_T|$, ϕ_p, $|\boldsymbol{k}_T|$, ϕ_k values
  - Includes both pseudo-scalar and dihadron SIDIS cross sections
- Guiding plans
  - Extreme flexibility
    - Allow many models for fragmentation and distribution functions
    - Various final states: pseudo-scalars, vector mesons, hadron pairs, etc.
    - Output options & connecting to analysis chains of various experiments
    - Minimize dependencies on other libraries
  - Full flavor and transverse momentum dependence.
- Current C++ package considered stable and allows further expansion
- Can be useful for both experimentalists and theorists.

$\pi^+\pi^0$ Kinematic Distributions, p.1

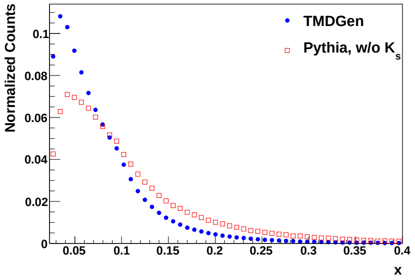

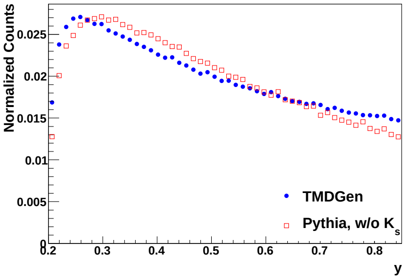

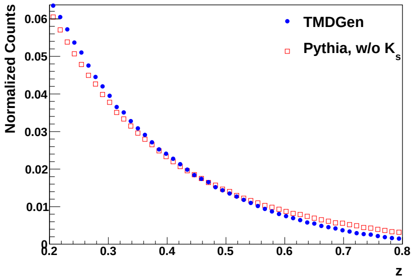

- Close agreement for x, y, z distributions.
- Main discrepancy in x distribution—most likely do to imbalance in the flavor contributions, or a subtle effects of Q^2 scaling.

$\pi^+\pi^0$ Kinematic Distributions, p.2

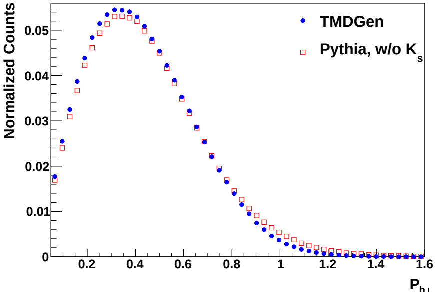

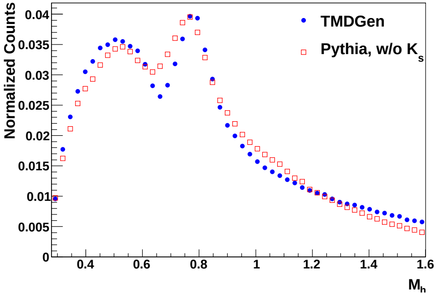

- Fairly good agreement in both $P_{h\perp}$ and M_h distributions.
- Note: some discrepancies in full $5D$ kinematic, but PYTHIA also doesn't match data in full $5D$

$\pi^+\pi^0$ Kinematic Distributions, Intrinsic Transverse Momentum

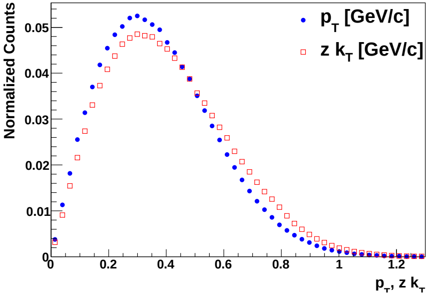

- Partonic transverse momentum denoted p_T
- The fragmenting quark's transverse momentum is zk_T
- Model requires $p_T \approx zk_T$ in order to get narrow $P_{h\perp}$ peak
- Model does not require any flavor dependence to k^2, k_T^2 cut-offs
- However, model poorly constrains RMS values $\langle p_T^2 \rangle$, $\langle k_T^2 \rangle$
- No other generator can give p_T, k_T distributions

Analysis

Neutral Pion Reconstruction

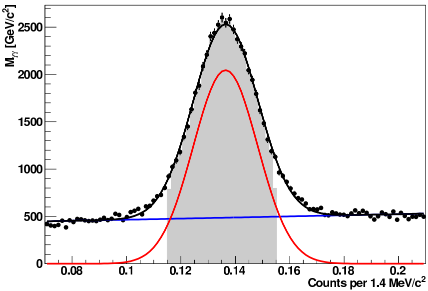

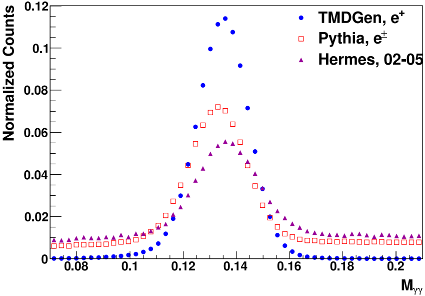

- Invariant mass spectrum of $\gamma\gamma$-system for $\pi^+\gamma\gamma$ events.
- $E_{\text{clus.}} = \alpha E_\gamma$, with α equal to 0.97, 0.9255 and 0.95 for HERMES, PYTHIA, and TMDGEN data, respectively.
- Central value of the peak is sufficiently close to the accepted value.
- Width of the peak is reflection of the resolution of the spectrometer for the π^0 mass.

Mass Distribution: $\pi^+\pi^0$

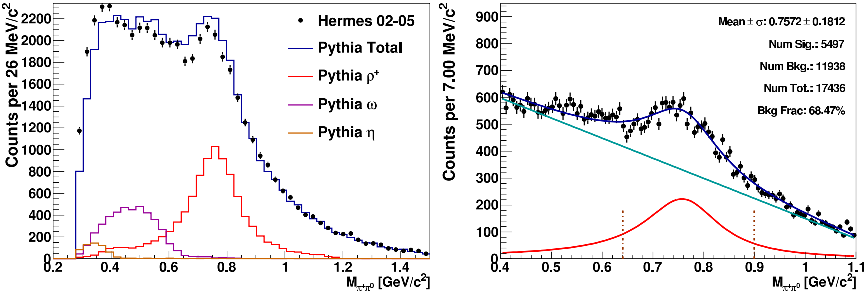

- Left panel: comparison with PYTHIA, highlighting various process decaying into $\pi^+\pi^-$ pair.
- Right panel: Hermes 02-05 data, fit to Breit-Wigner plus linear background to estimate background fraction.
- High background fraction, but hope only VMs in *pp*-wave.
- Distributions for other $\pi\pi$ dihadron effectively the same.

Mass Distribution: K^+K^-

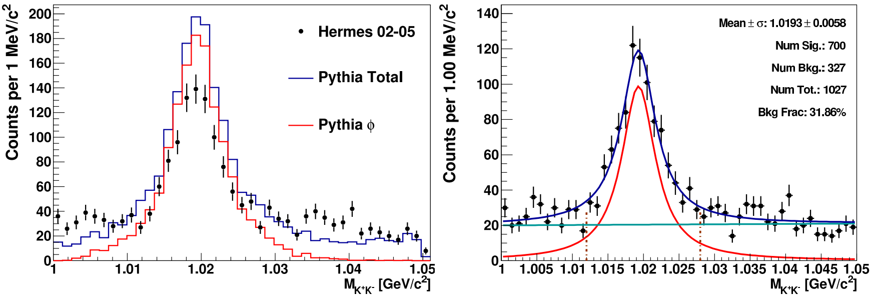

- Lower signal, but much lower background fraction.
- No other mesons decaying into K^+K^- within mass window.
- Clean access to strange quark distribution and fragmentation functions.

Fitting Functions

- Perform angular fit in each kinematic bin
- Main focus is on transverse target Collins and Sivers moments
- Fit function includes 41 angular moments plus constant term
  - Unpolarized moments, twist-2 and twist-3 (24 moments)
  - The transverse target Collins and Sivers moments (18 moments)

$$f(\cos\vartheta,\phi_h,\phi_R,\phi_S) = \sum_{\ell=0}^{2}\Bigg[\sum_{m=0}^{\ell} a_1^{|\ell,m\rangle} P_{\ell,m}\cos(m\phi_h - m\phi_R)$$
$$+\sum_{m=-\ell}^{\ell}\left(a_2^{|\ell,m\rangle} P_{\ell,m}\cos((2-m)\phi_h + m\phi_R) + a_3^{|\ell,m\rangle} P_{\ell,m}\cos((1-m)\phi_h + m\phi_R)\right)$$
$$+\sum_{m=-\ell}^{\ell}\left(b_1^{|\ell,m\rangle} P_{\ell,m}\sin((m+1)\phi_h - m\phi_R - \phi_S) + b_2^{|\ell,m\rangle} P_{\ell,m}\sin((1-m)\phi_h + m\phi_R + \phi_S\right.$$

- Constrain $a_1^{|0,0\rangle} = 1$.
- Fit parameters are integrals of structure functions, which are integrals of distribution and fragmentation functions

$$a_1^{|\ell,m\rangle} \propto f_1 D_1^{|\ell,m\rangle} \qquad a_3^{|\ell,m\rangle} \propto f_1 D_1^{|\ell,m\rangle}, h_1^{\perp} H_1^{\perp|\ell,m\rangle} \qquad b_1^{|\ell,m\rangle} \propto f_{1T}^{\perp} D_1^{|\ell,m\rangle}$$
$$a_2^{|\ell,m\rangle} \propto h_1^{\perp} H_1^{\perp|\ell,m\rangle} \qquad b_2^{|\ell,m\rangle} \propto h_1 H_1^{\perp|\ell,m\rangle}$$

Monte Carlo "Challenge A"

- Need Monte Carlo challenge to test efficacy of acceptance correction
- To act as "HERMES" data
  - TMDGEN data, generated with no dependence on $\cos\vartheta$ or on the azimuthal angles
  - Weight events using angular portion of the cross section (from TMDGEN) to induce angular dependence
- To act as "Monte Carlo" data (for acceptance correction)
  - Again, TMDGEN data generated with no angular dependence
- Compare results
  1. MLE fit of weighted TMDGEN data in 4π
  2. Acceptance correction ISE fit applied to weighted TMDGEN data within HERMES acceptance

Challenge A Results: Collins $|2,2\rangle$ $\pi^+\pi^0$

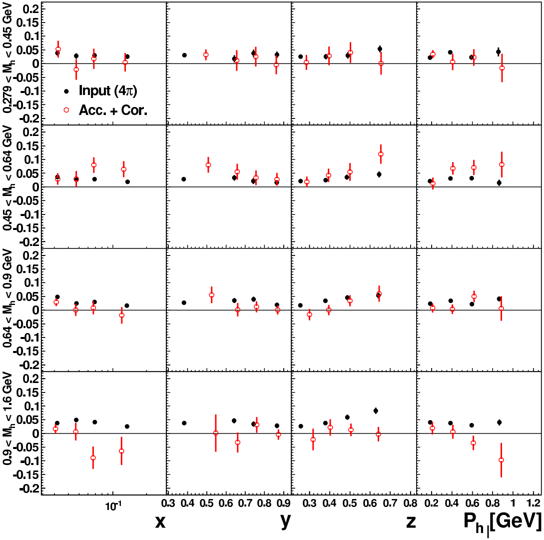

- As a representative moment, above is shown the $|2,2\rangle$ Collins moment for $\pi^+\pi^0$ dihadrons.

Challenge A Results: $\pi^+\pi^0$ χ^2/ndf Statistics

Moment	χ^2/ndf per Binning Option				
	M_h	M_h-x	M_h-y	M_h-z	M_h-$P_{h\perp}$
Sivers $\|0,0\rangle$	24.262	7.933	7.442	26.445	11.041
Sivers $\|1,-1\rangle$	4.130	1.798	1.501	1.423	1.368
Sivers $\|1,0\rangle$	32.172	40.630	17.661	50.027	11.113
Sivers $\|1,1\rangle$	2.105	1.335	1.259	0.842	1.038
Sivers $\|2,-2\rangle$	2.267	1.055	1.516	1.505	1.073
Sivers $\|2,-1\rangle$	1.558	3.525	3.379	7.401	4.048
Sivers $\|2,0\rangle$	206.813	63.409	59.620	201.947	65.524
Sivers $\|2,1\rangle$	3.309	2.847	3.466	30.484	4.804
Sivers $\|2,2\rangle$	1.851	1.047	1.668	0.785	1.426
Collins $\|0,0\rangle$	11.510	6.359	4.172	15.407	7.394
Collins $\|1,-1\rangle$	1.947	1.501	1.109	0.610	1.487
Collins $\|1,0\rangle$	67.696	63.585	19.607	15.370	25.493
Collins $\|1,1\rangle$	5.863	1.851	1.835	1.423	2.025
Collins $\|2,-2\rangle$	0.392	1.108	1.012	1.041	0.393
Collins $\|2,-1\rangle$	2.708	2.208	3.038	21.793	1.687
Collins $\|2,0\rangle$	49.310	33.906	18.686	125.888	18.458
Collins $\|2,1\rangle$	5.632	2.865	1.766	8.277	3.025
Collins $\|2,2\rangle$	3.906	1.857	1.157	1.787	1.854

- The χ^2/ndf is per each moment and binning choice, but over all the bins
- As a representative case, above are the χ^2/ndf statistics for $\pi^+\pi^0$ dihadrons.
- In general, the 2D binning yields better results than the 1D binning.
- The $|\ell,0\rangle$ moments are reconstructed quite poorly—but this is where acceptance is the worst.

Non-resonant Photon Pairs

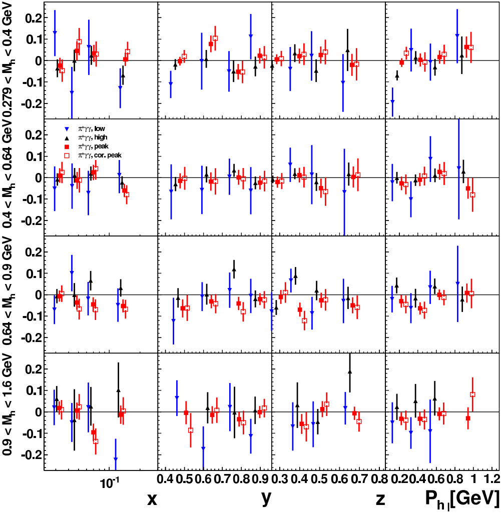

The Collins $|2,2\rangle$ moments for $\pi^+\pi^0$ dihadrons

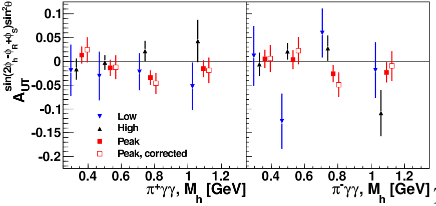

Collins $|2,2\rangle$ moments for $\pi^+\pi^0$ dihadrons vs. $M_{\gamma\gamma}$ regions

- Exists about a 25% background of non-resonant photon pairs
- Data from higher and lower $M_{\gamma\gamma}$ regions are fit to interpolate the background asymmetry in the π^0 peak region.
- The effect of subtracting this background is not large

Charge Symmetric Background

- Some candidate DIS leptons actually from processes generating e^+e^- pairs.
- Can use data where lepton has opposite charge as the beam to estimate bkg.
- Little data, but within statistical uncertainty, the background asymmetry appears negligible.

Year	$\pi^+\pi^0$		$\pi^+\pi^-$		$\pi^-\pi^0$		K^+K^-	
2002	222	5.0%	827	3.8%	145	4.3%	2	1.1%
2003	120	4.9%	477	3.9%	74	3.8%	1	1.0%
2004	762	5.0%	2849	3.9%	487	4.2%	4	0.7%
2005	1608	4.7%	7346	4.5%	1667	6.4%	18	1.4%
Total	2712	4.9%	11499	4.3%	2373	5.5%	25	1.2%

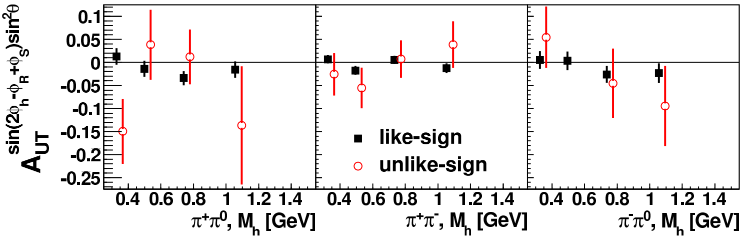

Exclusive Background

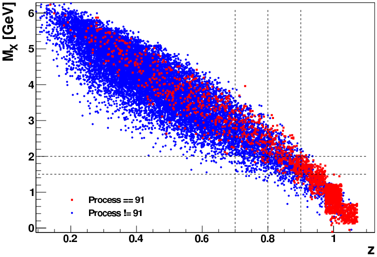

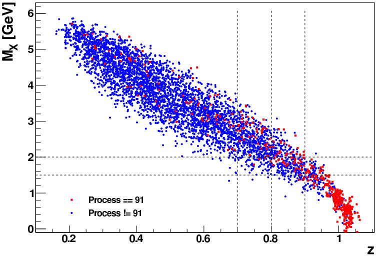

- Left panel, $\pi^+\pi^-$; right panel, K^+K^-.
- Comparison based on PYTHIA production tuned to HERMES kinematics, within HERMES acceptance
- Good background suppression ($\approx 3.5\%$) by limiting $z < 0.8$
- Missing mass (M_X) cut reduces statistics, but does not reduce background fraction

Vector Meson Fraction

Dihadron	Est. VM Stats.	Bkg. Frac.
$\pi^+\pi^0$	5497	68.5%
$\pi^+\pi^-$	10846	85.4%
$\pi^-\pi^0$	2774	77.9%
K^+K^-	700	31.9%

- Some partial waves, such as $|2, \pm 2\rangle$, are a simple sum of vector meson plus non-vector meson contributions
- Other partial waves involving interference, such as $|1, 1\rangle$, cannot be separated into a sum.
- For the $|2, \pm 2\rangle$ partial waves, one can consider isolating the vector meson contribution using the estimated background fractions.
- The fractions are determined by a Breit-Wigner plus linear background fit to the M_h distribution.

Comparison with Published Results

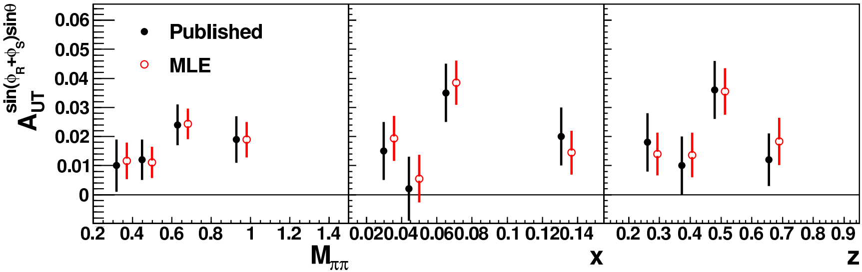

- As a general consistency check, the raw (not corrected) moments from an MLE fit to the data are compared with the published results.
- The binning is the same for both methods, though the fitting methods are different.
- The comparison is sufficiently good.

Systematic Studies

Monte Carlo "Challenge B"

- Very similar to Challenge A
- Challenge B, however, uses PYTHIA (including RADGEN) to act as data
- Thus estimated systematic includes both smearing and acceptance
- Also, use of different generators insures no "lucky" cancellations due to the cross sections being identical
- Systematic uncertainty is estimated as half the difference between the results from MLE fit of weighted PYTHIA 4π data and from acceptance correction fit of weighted PYTHIA (w/ RADGEN) within acceptance.

Challenge B Results: Collins $|2,2\rangle$ $\pi^+\pi^0$

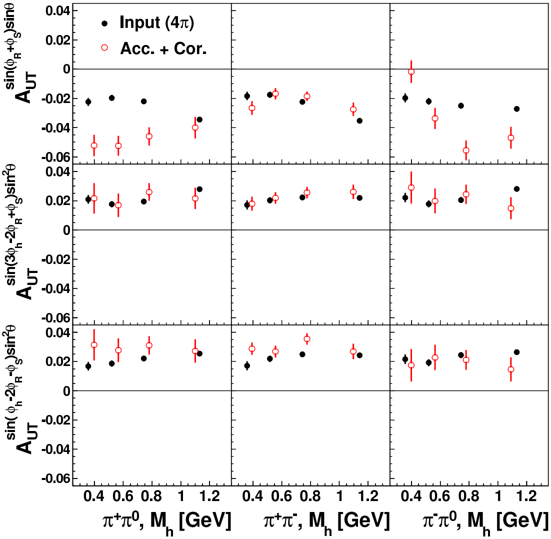

- As representative moments, above is shown the $|1,1\rangle$, $|2,-2\rangle$ and $|2,2\rangle$ Collins moment for pion-pair dihadrons versus M_h.

Challenge B Results: $\pi^+\pi^0$ χ^2/ndf Statistics

Moment	χ^2/ndf per Binning Option				
	M_h	M_h-x	M_h-y	M_h-z	M_h-$P_{h\perp}$
Sivers $\|0,0\rangle$	10.257	6.154	5.898	6.199	6.886
Sivers $\|1,-1\rangle$	8.649	2.064	1.872	2.681	3.024
Sivers $\|1,0\rangle$	38.928	48.047	27.105	59.303	16.620
Sivers $\|1,1\rangle$	1.072	1.729	2.029	1.393	1.549
Sivers $\|2,-2\rangle$	8.710	1.312	2.256	1.948	2.242
Sivers $\|2,-1\rangle$	14.156	7.346	5.586	11.712	5.233
Sivers $\|2,0\rangle$	191.392	81.096	46.959	106.730	80.811
Sivers $\|2,1\rangle$	9.984	1.987	6.877	4.140	4.155
Sivers $\|2,2\rangle$	1.746	0.987	0.993	1.409	1.403
Collins $\|0,0\rangle$	12.917	5.923	9.475	24.251	6.392
Collins $\|1,-1\rangle$	0.806	1.851	1.135	2.099	2.088
Collins $\|1,0\rangle$	47.455	31.840	37.332	45.703	20.431
Collins $\|1,1\rangle$	16.554	2.497	3.843	4.319	3.131
Collins $\|2,-2\rangle$	0.605	1.011	0.465	0.569	1.363
Collins $\|2,-1\rangle$	12.480	2.694	2.772	14.441	3.673
Collins $\|2,0\rangle$	33.781	32.088	28.132	174.760	16.624
Collins $\|2,1\rangle$	3.693	2.127	2.664	10.043	1.161
Collins $\|2,2\rangle$	1.596	0.740	1.227	1.364	1.048

- As a representative case, above are the χ^2/ndf statistics for $\pi^+\pi^0$ dihadrons.
- Same general trends as before
- Agreement is worse, due to using two generators and also due to including smearing effects.
- The $|2,\pm2\rangle$ Collins moments are still reconstructed quite well.

Year Dependence

- Data with both positron (2002-2004) and electron (2005) beams is combined for final sample
- Though SIDIS cross section invariant with respect to beam charge, systematic effects are not.
- Study 1
  - Compare the results from the combined fit versus results from combining the separate fit results
  - Very close agreement
- Study 2
  - Compare corrected 2002-2004 results with corrected 2005 results
  - Agreement not as good.
  - Systematic uncertainty is estimated as half the uncertainty needed to reduce the χ^2 per moment per bin to 1.

$$\delta A_{year} = \frac{1}{4}\sqrt{\left(A_e - A_p\right)^2 - \delta^2 A_e - \delta^2 A_p} \approx \frac{1}{4}\left|A_e - A_p\right|.$$

Year Dependence Study 2: Pion-Pair Dihadrons

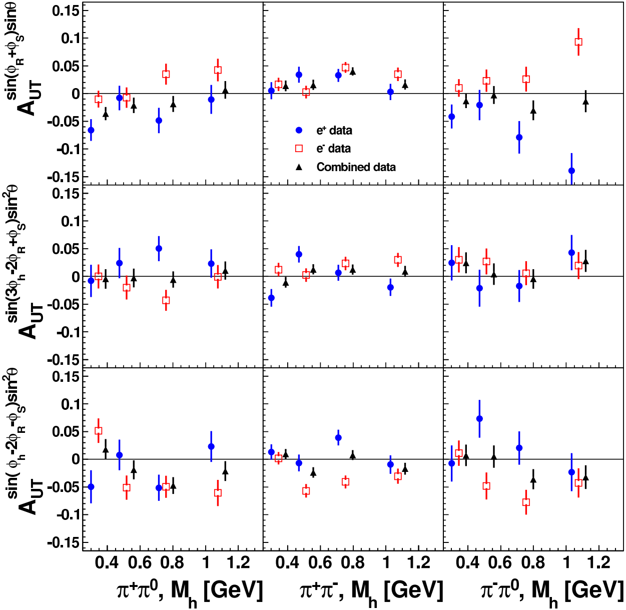

- The $|1,1\rangle$, $|2,-2\rangle$ and $|2,2\rangle$ Collins moments vs. M_h for each pion-pair dihadron.
- Fluctuations appear mostly random.

Particle Identification Procedure

- Two methods exist for assigning particle identification
  1. Assign the identification with the highest probability
  2. Assign all identifications to each event, but with varying weights
- Weights for second method computed according to
  - Define $P_{i,j} = p(ID_i|ID_j)$, where ID_j is the true identification and ID_i is the identification given by method 1.
  - For a given event, let ID_{i^*} be the identification given by method 1.
  - Weight for the event being ID_j is then P^{-1}_{j,i^*}.
- These methods are part of the HERMES standard operating procedure.
- A systematic uncertainty is assigned, equal to half the difference between the two methods.

Comparison of Particle Identification Procedures: $\pi\pi$ Dihadrons

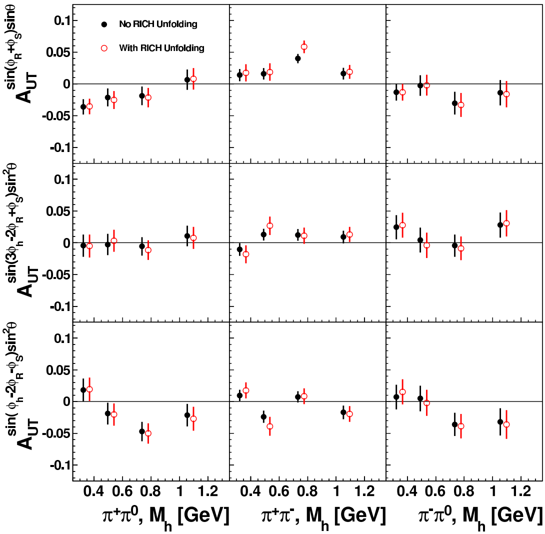

Comparison of Particle Identification Procedures: K^+K^- Dihadrons

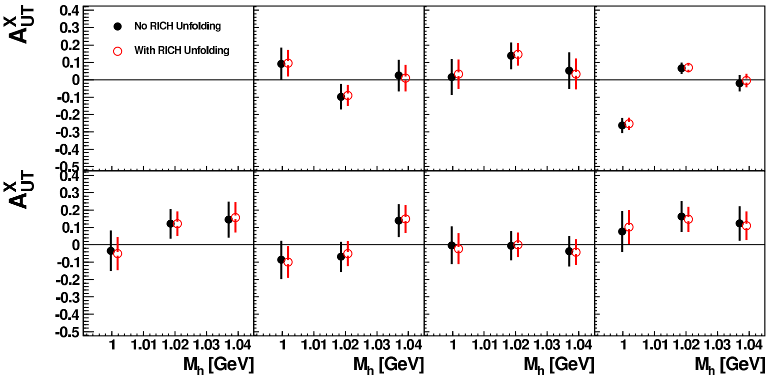

- Sivers moments for K^+K^-, panels arranged as before.
- Very little difference seen between the identification procedures.

Combined Systematic Uncertainty

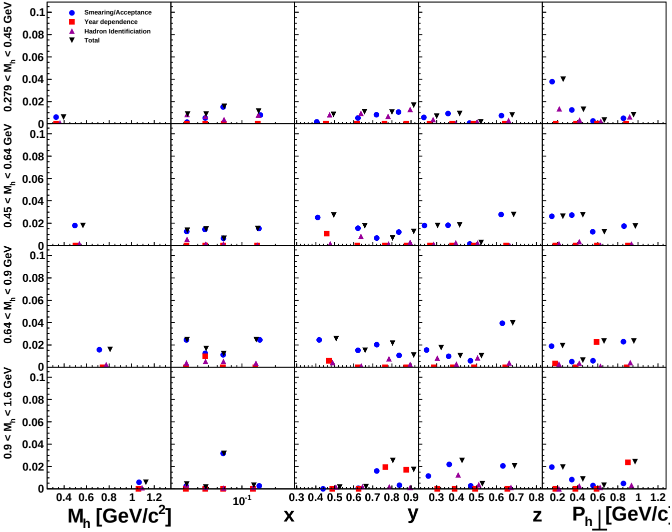

- Representative plot for the comparison of sources and combined systematic uncertainties: the $|2,2\rangle$ Collins moment for $\pi^+\pi^0$ dihadrons.

Results and Conclusions

Sivers moments for K^+K^- Dihadrons

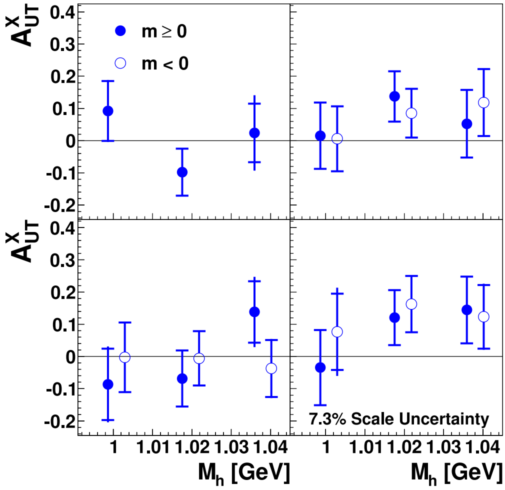

- Panels, clockwise from upper left, are for the $|0,0\rangle$, $|1,\pm1\rangle$, $|2,\pm2\rangle$, $|2,\pm1\rangle$ partial waves.
- Sivers moments for ϕ-meson related to orbital angular momentum of the gluons.
- No clear difference in ϕ-meson M_h peak region (center bin) versus outside bins.
- Other, more direct measurements indicate gluon orbital angular momentum small
- These results are consistent with small gluon orbital angular momentum.

Collins $|1,1\rangle$ Comparison with Published Results

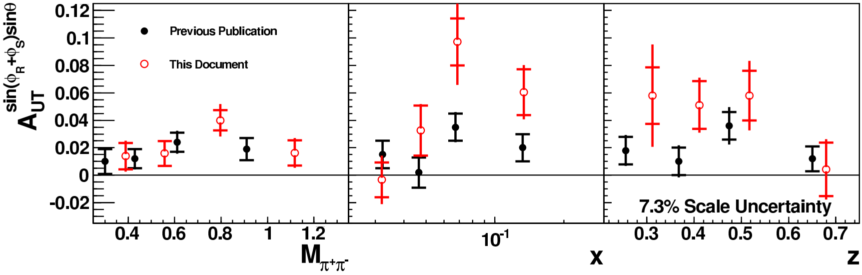

- Note: binning is not consistent between results being compared.
- New results generally consistent, with slightly larger moments in the ρ meson mass peak region.

Collins $|1, 1\rangle$ New Results

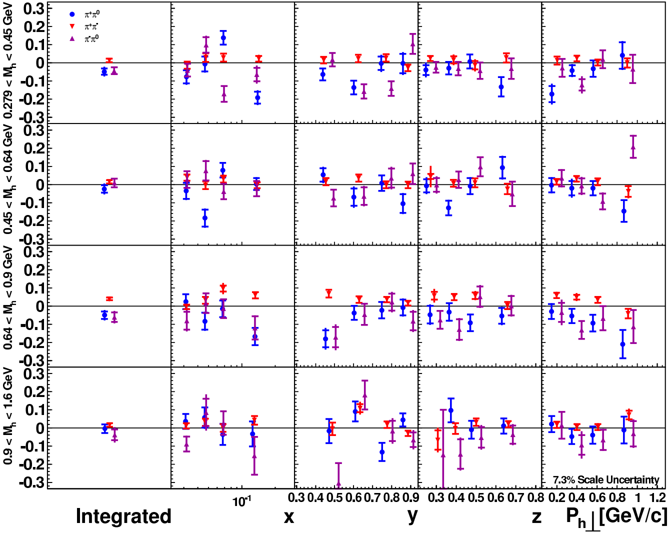

- Much more information now available
- Will be useful in a global extraction of transversity.

Select Collins Moments vs. Invariant Mass

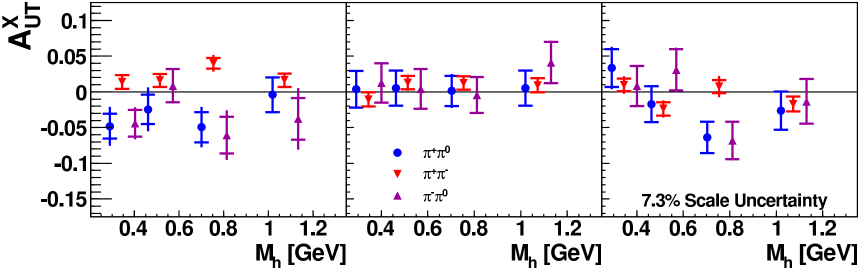

- The $\pi^+\pi^0$ moments tend to be quite similar to the $\pi^-\pi^0$ moments.
- The $\pi^\pm\pi^0$ dihadron $|1, 1\rangle$ Collins moments are larger in magnitude and have opposite sign than the comparable $\pi^+\pi^-$ dihadron moments.
- The $|2, -2\rangle$ Collins moments consistent with zero for all pion-pair dihadrons and in all mass bins.
  - Can be explained by assuming transversity distribution function fixes fragmenting quark to be in the $|\frac{1}{2}, \frac{1}{2}\rangle$ state.
- The $|2, 2\rangle$ Collins moment consistent with zero in all bins except the ρ mass peak M_h bin for $\pi^\pm\pi^0$ dihadrons.

Collins $|2,2\rangle$ Kinematic Dep.

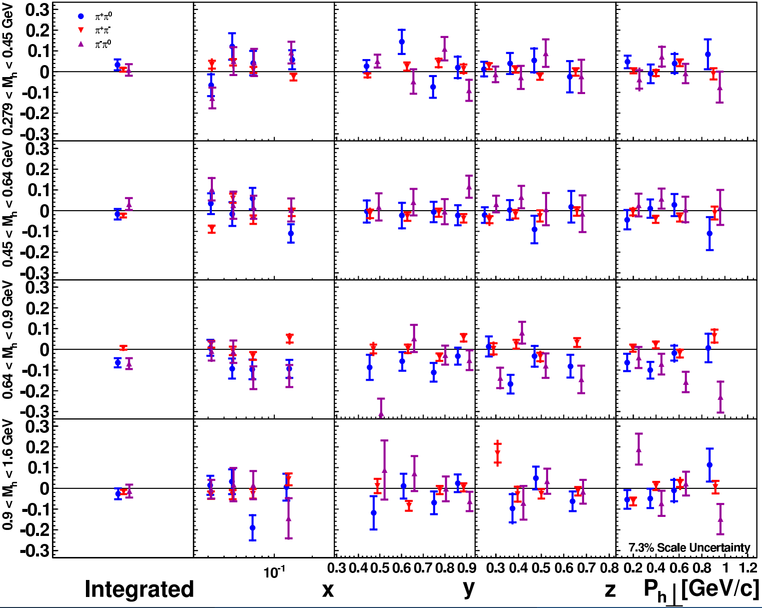

ρ Meson Collins $|2, 2\rangle$ Results

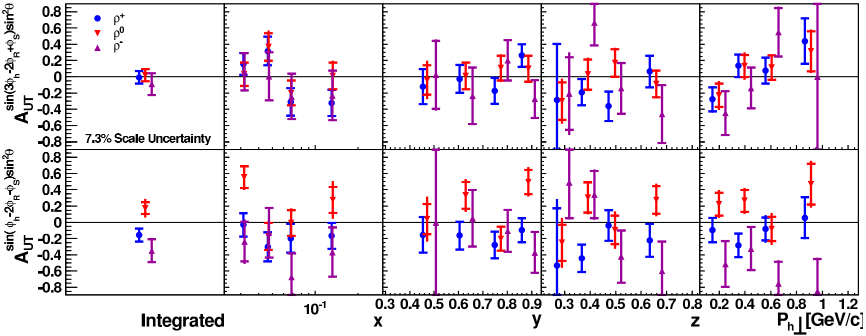

- Top row are $|2, -2\rangle$ Collins moments; bottom row are $|2, 2\rangle$ Collins moments.
- Note significantly larger scale than earlier plots.
- Kinematic dependencies poorly constrained, but results versus M_h clearly indicate the sign of the moments.
- Sign of the results consistent with expectations from the Lund/Artru and gluon radiation models.

Conclusions

- Non-collinear SIDIS Dihadron production provides unique access to
  - Strange quark distribution and fragmentation functions
  - Testing the Lund/Artru model
  - The TMD spin structure of fragmentation
- Theoretical developments include
  - Clarifying the prediction of the Lund/Artru Model
  - Developing the gluon radiation model
  - Defining a new partial wave expansion
  - Computing the twist-3 dihadron cross section
- Numerical Methods and Software
  - Smearing and acceptance correction method
  - TMDGEN Monte Carlo generator
- Analysis and systematic studies completed
- Results are in agreement with Lund/Artru model and the gluon radiation model, assuming u-quark dominance
- This dissertation forms the basis for upcoming release of preliminary results by the HERMES Collaboration

Backup Slides

Rigorous Definitions

- Fragmentation Correlation Matrix

$$\Delta_{mn}(P_h, S_h; k) \quad = \quad \sum_X \int \frac{d^4x}{(2\pi)^4} e^{ip\cdot x} \langle 0 | \Psi_m(x) | P_h, S_h; X \rangle \langle P_h, S_h; X | \overline{\Psi}_n(0) | 0 \rangle$$

- Trace Notation

$$\Delta^{[\Gamma]}(z, M_h, |\boldsymbol{k}_T|, \cos\vartheta, \phi_R - \phi_k) \quad = \quad 4\pi \frac{z|\boldsymbol{R}|}{16M_h} \int dk^+ \, \mathrm{Tr}\left[\Gamma \Delta(k, P_h, R)\right] \Big|_{k^- = P_h^-/z}.$$

- Define fragmentation functions via trace relations

FF	Previous Definitions Pseudo-Scalar	 Dihadron	New Definition All Final States
D_1	$\Delta^{[\gamma^-]}$	$\Delta^{[\gamma^-]}$	$\Delta^{[\gamma^-(1+i\gamma^5)]}$
$G_1^\perp$	$--$	$\propto \Delta^{[\gamma^-\gamma^5]}$	$--$
$H_1^\perp$	$\Delta^{[(\sigma^{1-})\gamma^5]}$	$\Delta^{[(\sigma^{1-})\gamma^5]}$	$\Delta^{[(\sigma^{1-}+i\sigma^{2-})\gamma^5]}$
$\bar{H}_1^{\measuredangle}$	$--$	$\propto \Delta^{[(\sigma^{2-})\gamma^5]}$	$--$

- Real part of fragmentation function similar
- New definition of D_1 & $H_1^\perp$
  - Adds "imaginary" part to D_1 & $H_1^\perp$, instead of introducing new functions.
  - Functions are complex valued and depend on Q^2, z, $|k_T|$, M_h, $\cos\vartheta$, $(\phi_R - \phi_k)$.

Further Comments on Partial Wave Expansion

- Previously studied $H_{1,UT}^{\perp sp}$ not pure *sp*-interference, but also *pp*-interference
- In fact, $H_{1,UT}^{\perp sp} \propto H_1^{\perp|1,1\rangle}$
- Typical $SU(2)$ selection rules yield necessary condition for a partial waves surviving in collinear case
  - Moments with $h_1 H_1^{\perp|\ell,m\rangle}$ (Collins moments)
    - h_1 has $\Delta m = 0$.
    - Collins has $\chi \neq \chi'$, and $\Delta m = -1$.
    - Fragmentation functions surviving in collinear case must have $m = 1$ so $\sum m = 0$.
    - Collinear moments are $|1,1\rangle$, $|2,1\rangle$.
  - Moments with $h_1^{\perp} H_1^{\perp|\ell,m\rangle}$ (Boer-Mulders moments)
    - $h_1^{\perp}$ has $\Delta m = -1$.
    - Collins has $\chi \neq \chi'$, and $\Delta m = -1$.
    - Moments surviving in collinear case have $m = 2$, i.e. $|2,2\rangle$.
- One can extrapolate the twist-3 dihadron cross section from pseudo-scalar cross section
  - Large computational advantage
  - For clean analysis, important to understand twist-3 moments
  - Twist-3 moments can contribute to twist-2 moments through acceptance effects

Relations with Previous Notation, Non-expanded

- Comparing with similar trace definitions, e.g. PRD 67:094002 yields the relations

$$D_1\Big|_{Gliske} = \left[D_1 + i\frac{|\boldsymbol{R}||\boldsymbol{k}_T|}{M_h^2}\sin\vartheta\sin(\phi_R-\phi_k)\,G_1^{\perp}\right]_{other}, \quad (1)$$

$$H_1^{\perp}\Big|_{Gliske} = \left[H_1^{\perp} + \frac{|\boldsymbol{R}|}{|\boldsymbol{k}_T|}\sin\vartheta e^{i(\phi_R-\phi_k)}\,\bar{H}_1^{\sphericalangle}\right]_{other} = \frac{|\boldsymbol{R}|^2}{|\boldsymbol{k}_T|^2}H_1^{\sphericalangle}\Big|_{other}, \quad (2)$$

$$(3)$$

- Inconsistencies in the literature between definitions of $H_1^{\sphericalangle}, \bar{H}_1^{\sphericalangle}, H_1'^{\sphericalangle}$.

Relations with Previous Notation, Partial Waves

$$
\begin{aligned}
D_1^{|0,0\rangle} &= D_{1,OO} = \left(\frac{1}{4}D^s_{1,OO} + \frac{3}{4}D^p_{1,OO}\right), \\
D_1^{|1,0\rangle} &= D_{1,OL}, \\
D_1^{|1,\pm1\rangle} &= D_{1,OT} \mp \frac{|\boldsymbol{k}_T|\,|\boldsymbol{R}|}{M_h^2} G^{\perp}_{1,OT}, \\
D_1^{|2,0\rangle} &= \frac{1}{2}D_{1,LL}, \\
D_1^{|2,\pm1\rangle} &= \frac{1}{2}\left(D_{1,LT} \mp \frac{|\boldsymbol{k}_T|\,|\boldsymbol{R}|}{M_h^2} G^{\perp}_{1,LT}\right), \\
D_1^{|2,\pm2\rangle} &= D_{1,TT} \mp \frac{1}{2}\frac{|\boldsymbol{k}_T|\,|\boldsymbol{R}|}{M_h^2} G^{\perp}_{1,TT},
\end{aligned}
$$

$$
\begin{aligned}
H_1^{\perp\,|0,0\rangle} &= H^{\perp}_{1,OO} = \frac{1}{4}H^{\perp s}_{1,OO} + \frac{3}{4}H^{\perp p}_{1,OO}, \\
H_1^{\perp\,|1,1\rangle} &= H^{\perp}_{1,OT} + \frac{|\boldsymbol{R}|}{|\boldsymbol{k}_T|}\bar{H}^{\sphericalangle}_{1,OT} = \frac{|\boldsymbol{R}|}{|\boldsymbol{k}_T|}H^{\sphericalangle}_{1,OT} \\
H_1^{\perp\,|1,0\rangle} &= H^{\perp}_{1,OL}, \\
H_1^{\perp\,|1,-1\rangle} &= H^{\perp}_{1,OT}, \\
H_1^{\perp\,|2,2\rangle} &= H^{\perp}_{1,TT} + \frac{|\boldsymbol{R}|}{|\boldsymbol{k}_T|}\bar{H}^{\sphericalangle}_{1,TT} = \frac{|\boldsymbol{R}|}{|\boldsymbol{k}_T|}H^{\sphericalangle}_{1,TT} \\
H_1^{\perp\,|2,1\rangle} &= \frac{1}{2}H^{\perp}_{1,LT} + \frac{1}{2}\frac{|\boldsymbol{R}|}{|\boldsymbol{k}_T|}\bar{H}^{\sphericalangle}_{1,LT} = \frac{1}{2}\frac{|\boldsymbol{R}|}{|\boldsymbol{k}_T|}H^{\sphericalangle}_{1,LT} \\
H_1^{\perp\,|2,0\rangle} &= \frac{1}{2}H^{\perp}_{1,LL}, \\
H_1^{\perp\,|2,-1\rangle} &= \frac{1}{2}H^{\perp}_{1,LT}, \\
H_1^{\perp\,|2,-2\rangle} &= H^{\perp}_{1,TT}.
\end{aligned}
$$

Fragmentation Correlation Function

- Described spectator model uses the following fragmentation correlation function

$$
\begin{aligned}
\Delta^q(k, P_h, R) \;=\; & \Big\{ |F^s|^2 \, e^{-2\frac{k^2}{\Lambda_s^2}} \not{k} \left(\not{k} - \not{P}_h + M_s\right) \not{k} \\
& + |F^p|^2 \, e^{-2\frac{k^2}{\Lambda_p^2}} \not{k}\not{R} \left(\not{k} - \not{P}_h + M_s\right) \not{R}\not{k} \\
& + F^{s*} F^p e^{-2\frac{k^2}{\Lambda_{sp}^2}} \not{k} \left(\not{k} - \not{P}_h + M_s\right) \not{R}\not{k} \\
& + F^s F^{p*} e^{-2\frac{k^2}{\Lambda_{sp}^2}} \not{k}\not{R} \left(\not{k} - \not{P}_h + M_s\right) \not{k} \Big\} \\
& \times \frac{1}{(2\pi)^3} \frac{1}{k^4} \delta\left((k - P_h)^2 - M_s^2\right) e^{-2\frac{k_T^2}{\Lambda_b^2}} .
\end{aligned}
$$

Model Calculation for Fragmentation Functions

$$\frac{16\pi^2 M_h k^4}{|\boldsymbol{R}|} D_1^{|0,0\rangle} = \left(\frac{z^2|\boldsymbol{k}_T|^2 + M_s^2}{1-z}\right)\left[\left|F^s\right|^2 e^{-2\frac{k^2}{\Lambda_s^2}} - R^2\left|F^p\right|^2 e^{-2\frac{k^2}{\Lambda_p^2}}\right]$$

$$\frac{16\pi^2 M_h k^4}{|\boldsymbol{R}|} D_1^{|1,1\rangle} = -2M_s|\boldsymbol{R}||\boldsymbol{k}_T|\left[\mathrm{Re}\left(F^{s*}F^p\right) e^{-2\frac{k^2}{\Lambda_{sp}^2}}\right]$$

$$\frac{16\pi^2 M_h k^4}{|\boldsymbol{R}|} D_1^{|1,0\rangle} = -2\frac{M_s|\boldsymbol{R}|}{zM_h}\left(M_h^2 + z^2|\boldsymbol{k}_T|^2\right)\left[\mathrm{Re}\left(F^{s*}F^p\right) e^{-2\frac{k^2}{\Lambda_{sp}^2}}\right]$$

$$\frac{16\pi^2 M_h k^4}{|\boldsymbol{R}|} D_1^{|2,2\rangle} = |\boldsymbol{k}_T|^2|\boldsymbol{R}|^2\left[\left|F^p\right|^2 e^{-2\frac{k^2}{\Lambda_p^2}}\right],$$

$$\frac{16\pi^2 M_h k^4}{|\boldsymbol{R}|} D_1^{|2,1\rangle} = \frac{|\boldsymbol{k}_T||\boldsymbol{R}|^2}{zM_h}\left(M_h^2 + z^2|\boldsymbol{k}_T|^2 + \frac{1}{2}z^2k^2\right)\left[\left|F^p\right|^2 e^{-2\frac{k^2}{\Lambda_p^2}}\right],$$

$$\frac{16\pi^2 M_h k^4}{|\boldsymbol{R}|} D_1^{|2,0\rangle} = \left(\frac{|\boldsymbol{R}|^2}{z^2M_h^2}\left(M_h^2 + z^2|\boldsymbol{k}_T|^2\right)\left(M_h^2 + z^2|\boldsymbol{k}_T|^2 + z^2k^2\right) - 2|\boldsymbol{k}_T|^2|\boldsymbol{R}|^2\right)\left[\left|F^p\right|^2 e^{-2\frac{k^2}{\Lambda_p^2}}\right],$$

$$D_1^{|\ell,-m\rangle} = D_1^{|\ell,m\rangle}.$$

Model Calculation for Fragmentation Functions

$$\frac{8\pi^2 k^4}{|\boldsymbol{R}|} H_1^{\perp|1,1\rangle} = -\frac{|\boldsymbol{R}|}{|\boldsymbol{k}_T|}\left(k^2 + |\boldsymbol{k}_T|^2\right)\left(\left(1 - z^2\right) k^2 - z^2 |\boldsymbol{k}_T|^2\right) \times \left[\mathrm{Im}\left(F^{s*} F^p\right) e^{-2\frac{k^2}{\Lambda_{sp}^2}}\right],$$

$$\frac{8\pi^2 k^4}{|\boldsymbol{R}|} H_1^{\perp|1,0\rangle} = \frac{1}{z} M_h |\boldsymbol{R}| \left(z k^2 - 2\left(M_h^2 + z^2 (k^2 + |\boldsymbol{k}_T|^2)\right)\right) \times \left[\mathrm{Im}\left(F^{s*} F^p\right) e^{-2\frac{k^2}{\Lambda_{sp}^2}}\right],$$

$$\frac{8\pi^2 k^4}{|\boldsymbol{R}|} H_1^{\perp|1,-1\rangle} = -M_h^2 |\boldsymbol{R}||\boldsymbol{k}_T| \left[\mathrm{Im}\left(F^{s*} F^p\right) e^{-2\frac{k^2}{\Lambda_{sp}^2}}\right].$$